research papers

Piezoelectric coefficients d_{14}, d_{16}, d_{34} and d_{36} of an L-arginine hydrochloride monohydrate crystal by X-ray three-beam diffraction

Juliana M. A. Almeida,[a] Marcus A. R. Miranda,[b]* Luis H. Avanci,[c] Alan S. de Menezes,[d] Lisandro P. Cardoso[c] and José M. Sasaki[a]

[a]Departamento de Física, Universidade Federal do Ceará, CP 6030, 60455-760 Fortaleza, CE, Brazil, [b]Department of Physics, University of Guelph, Guelph, ON, Canada N1G 2W1, [c]Instituto de Física, Universidade de São Paulo, CP 66318, 05315-970 São Paulo, SP, Brazil, and [d]Instituto de Física Gleb Wataghin, UNICAMP, CP 6165, 13083-970 Campinas, SP, Brazil.
E-mail: marcus@physics.uoguelph.ca

Previous work employed X-ray three-beam diffraction techniques to obtain part of the L-arginine hydrochloride monohydrate (L-AHCL.H$_2$O) piezoelectric coefficients, namely d_{21}, d_{22}, d_{23} and d_{25}. Those coefficients were obtained by measuring the shift in the angular position of a number of secondary reflections as a function of the electric field applied in the [010] piezoelectric direction. In this paper a similar procedure has been used to measure the remaining four piezoelectric coefficients in L-AHCL.H$_2$O: with the electric field applied in the [100] direction, d_{14} and d_{16} were measured; with the electric field applied in the [001] direction, d_{34} and d_{36} were obtained. Therefore the entire piezoelectric matrix of the L-AHCL.H$_2$O crystal has been successfully measured.

Keywords: X-ray diffraction; strain-induced piezoelectric fields; arginine; piezoelectric materials.

1. Introduction

After the discovery of L-arginine phosphate monohydrate (Xu *et al.*, 1983), a non-linear optical material for the frequency conversion of Nd:YAG lasers, Monaco *et al.* (1987) synthesized ten other salts of L-arginine which also had non-linear optical properties. L-Arginine hydrochloride monohydrate (C$_6$H$_{14}$N$_4$O$_2$HCl.H$_2$O, L-AHCL) was one of those non-linear optical materials and several of its physical and non-linear optical properties have been extensively discussed (Monaco *et al.*, 1987; Deloach, 1994; Evlanova *et al.*, 1990; Rashkovich & Shekunov, 1991; Haussuehl *et al.*, 1990).

Crystals of L-AHCL belong to the group of the semi-organic crystals with non-linear optical properties (Mukerji & Kar, 1998; Petrosyan *et al.*, 2000) in which the L-arginine molecule is present in the form of a dipolar ion (zwitterion). This crystal crystallizes in a monoclinic structure with space group $P2_1$, having therefore piezoelectric properties. Its unit cell (a = 11.044 Å, b = 8.481 Å, c = 11.214 Å and β = 91.31°; Dow & Jensen, 1970) has two molecules and the crystal polar axis is oriented along the crystallographic b axis.

Based on X-ray three-beam diffraction techniques, a versatile method was developed to allow the investigation of the electric field effect over any crystalline lattice (Almeida *et al.*, 2003; Avanci *et al.*, 1998, 2000; de Santos *et al.*, 2003). This method had its first successful application in the determination of the piezoelectric coefficients of the non-linear optical organic crystal mNA (meta-nitroaniline) and, since then, several other materials have been analyzed. MBAMP [(−)-2-(α)-methylbenzylaminonitropyridine], Rochelle salt and L-arginine hydrochloride monohydrate are examples of application of the method where the applied electric field was parallel to the crystal polar axes, which for all these materials is along the crystallographic b axis. In all these cases it was possible to determine the piezoelectric coefficients d_{21}, d_{22}, d_{23} and d_{25} (Almeida *et al.*, 2003; Avanci *et al.*, 2000; de Santos *et al.*, 2003).

In this paper, X-ray three-beam diffraction techniques were applied to study electric-field-induced triclinic distortions in the monoclinic L-AHCL.H$_2$O crystal. This is an extension of the procedure used in previous work (Almeida *et al.*, 2003), where now the electric field is applied perpendicular to the polar axis of the L-AHCL.H$_2$O crystal.

It is important to note that the piezoelectric coefficients of a very similar crystal, L-arginine hydrobromide monohydrate (L-AHBR.H$_2$O), are known (Haussuehl *et al.*, 1990). Haussuehl *et al.* (1990) did not find it necessary to measure the coefficients of L-AHCL.H$_2$O as well, assuming that they would be very close. However, a comparison with the values of our previous work (Almeida *et al.*, 2003) shows a significant difference. This can be attributed in part to the fact that L-AHBR.H$_2$O is softer than L-AHCL.H$_2$O (Mukerjia & Kar,

2000), probably because the hydrogen-bond strength between the chloride ion and the guanidyl group is greater than that between the bromide ion and the guanidyl group; however, a more detailed explanation is still needed. Therefore we believed that it was important to complete the piezoelectric characterization of L-AHCL.H$_2$O.

2. Theory

The application of a static (or quasi-static) electric field into a piezoelectric crystal induces small changes in the lattice parameters of the crystal, the well known converse piezoelectric effect (Nye, 1957). In the following, X, Y and Z represent the applied electric field directions forming an orthogonal set. Their relation with the crystallographic axes is as follows: Y and Z are parallel to the crystallographic b and c axes, respectively, while X is perpendicular to both Y and Z. The functions that relate the piezoelectric coefficients to the lattice parameters are shown below. These equations are applied for a triclinic distortion in a monoclinic structure and with the electric field applied in the X, Y and Z directions.

(i) Electric field applied in X,

$$\Delta\alpha = -d_{14}E_X, \tag{1}$$

$$\Delta\gamma = -\left[d_{16}\sin\beta + d_{14}\cos\beta\right]E_X. \tag{2}$$

(ii) Electric field applied in Y,

$$\frac{1}{E_Y}\frac{\Delta a}{a} = d_{21}\sin^2\beta + d_{23}\cos^2\beta + \frac{1}{2}d_{25}\sin(2\beta), \tag{3}$$

$$\frac{\Delta b}{b} = d_{22}E_Y, \tag{4}$$

$$\frac{\Delta c}{c} = d_{23}E_Y, \tag{5}$$

$$\frac{1}{E_Y}\Delta\beta = \frac{1}{2}(d_{21} - d_{23})\sin(2\beta) - d_{25}\sin^2\beta. \tag{6}$$

(iii) Electric field applied in Z,

$$\Delta\alpha = -d_{34}E_Z, \tag{7}$$

$$\Delta\gamma = -\left[d_{36}\sin\beta + d_{34}\cos\beta\right]E_Z. \tag{8}$$

In this paper we are concerned only with cases (i) and (iii) since the other was covered in previous work (Almeida *et al.*, 2003). Taking into account the above equations, all we need to do is measure the lattice parameter variations as a function of the electric field and then solve the systems of equations given by (1) and (2) for the piezoelectric coefficients d_{14} and d_{16}, and (7) and (8) for d_{34} and d_{36}.

The technique used to measure the small variations in the lattice parameters is three-beam diffraction. In the multiple-diffraction phenomenon a set of planes, parallel or not to the sample surface, referred to as primary planes ($h_{\rm p}$, $k_{\rm p}$, $l_{\rm p}$), are adjusted to diffract the incident beam. By rotating the crystal around the primary reciprocal lattice vector (φ axis), several other secondary planes ($h_{\rm s}$, $k_{\rm s}$, $l_{\rm s}$), with arbitrary orientation, within the single crystal also diffract the same incident beam. The interaction among the beams diffracted by the primary and the several secondary reflections are established by the coupling reflections ($h_{\rm p} - h_{\rm s}$, $k_{\rm p} - k_{\rm s}$, $l_{\rm p} - l_{\rm s}$). These interactions appear in the $I_{\rm primary}$ *versus* φ pattern which is usually called a Renninger scan (Renninger, 1937). The plot of the diffracted primary intensity as a function of the rotation angle φ is the Renninger scan that shows oscillations in the primary intensity as positive (*Umweganregung*) or negative (*Aufhellung*) peaks, depending upon whether the interaction between the primary and the secondary beams is constructive or destructive, respectively. Owing to both the n-fold symmetry of the chosen primary vector and the two diffraction conditions represented by the entrance and the exit of the secondary reciprocal lattice point on the Ewald sphere under rotation, the Renninger scan shows $2n$ mirrors of symmetry throughout the pattern. A detailed review of this technique has been given by Chang (1984).

It is important to note that the secondary reflection can have a completely different orientation when compared with the primary reflection; therefore one obtains three-dimensional information in a single Renninger scan. This is important when measuring different piezoelectric coefficients because now it is unnecessary to have crystals cut in special orientations. Furthermore, for a multiple-diffraction peak to occur, two reflections have to satisfy the Bragg condition at the same time, which makes the position of such a peak very sensitive to very small variations in the lattice parameters.

For a fixed wavelength λ, the angular position of a secondary multiple-diffraction peak corresponding to a general (h, k, l) secondary plane can be determined in terms of the angle $\varphi \pm \varphi_0$ (the '$\pm$' signal defines the entrance and exit of the reciprocal secondary node in the Ewald sphere), where φ_0 is the angle between the secondary vector (**H**) and the reference vector measured on the Ewald sphere equatorial plane (Cole *et al.*, 1962). This angular peak position is given by

$$\cos\left(\varphi^{hkl} \pm \varphi_0\right) = \frac{1}{2}\frac{H^2 - \mathbf{H}\cdot\mathbf{H}}{\left[(1/\lambda^2) - \left(H_0^2/4\right)\right]^{1/2}\left(H^2 - H_\parallel^2\right)^{1/2}}, \tag{9}$$

where $\mathbf{H}_0$ is the primary vector, $\mathbf{H}$ is the secondary vector defined as $\mathbf{H}_{hkl} = h\mathbf{a}^* + k\mathbf{b}^* + l\mathbf{c}^*$, and $\mathbf{H}_\parallel$ represents the component of $\mathbf{H}$ along $\mathbf{H}_0$ defined by

$$\mathbf{H}_\parallel = (\mathbf{H}\cdot\mathbf{H}_0)\,\mathbf{H}_0/H_0^2. \tag{10}$$

Therefore the angular position of a secondary ($h_{\rm s}$, $k_{\rm s}$, $l_{\rm s}$) multiple-diffraction peak is a function of the lattice parameters

$$\cos(\varphi^{hkl} \pm \varphi_0) = f(a, b, c, \alpha, \beta, \gamma). \tag{11}$$

When applying a small electric field in the X or Z directions [cases (i) and (iii)], according to the piezoelectric tensor, only the unit-cell angles α and γ will change. So it is possible to write

$$-\sin\left(\varphi^{hkl} \pm \varphi_0\right)\Delta\left(\varphi^{hkl} \pm \varphi_0\right) = \frac{\partial f(\alpha,\gamma)}{\partial\alpha}\Delta\alpha + \frac{\partial f(\alpha,\gamma)}{\partial\gamma}\Delta\gamma,$$

$$(12)$$

where the dependence with the other lattice parameters was omitted. The derivative parts in the equation above are easily calculated and the angles are obtained experimentally. In this way it is only necessary to measure the angular position shifts of any two multiple-diffraction peaks in order to solve the equation for the variation in the lattice parameters.

In order to confirm the coefficient d_{21}, already determined previously (Almeida *et al.*, 2003), symmetrical rocking curves were used, with the electric field applied in the $\mathbf{E} = E_Y\mathbf{y}$ direction.

From equations (3) and (6) the d_{21} coefficient can be obtained as

$$\frac{1}{E_Y}\left[\cot(\beta)\Delta\beta + \frac{\Delta a}{a}\right] = d_{21}.$$

$$(13)$$

Differentiating Bragg's law, one can determine $\Delta a/a$ following the steps

$$\lambda = 2d\sin\omega \rightarrow \lambda = (2a\sin\beta\sin\omega)/h,$$

where $d = (a\sin\beta)/h$, and finally

$$\frac{\Delta a}{a} = -\cot\left(\omega^{h00}\right)\Delta\omega^{h00} - \cot(\beta)\Delta\beta,$$

$$(14)$$

giving rise to the final expression of the desired coefficient. Combining equations (13) and (14) one arrives at

$$d_{21} = \frac{-\cot(\omega)\Delta\omega}{E_Y}.$$

$$(15)$$

3. Experimental procedure

L-Arginine hydrochloride monohydrate crystals have been grown by slow evaporation of an aqueous solution of commercial powder at controlled temperature. Single crystals of good optical quality (confirmed by the X-ray synchrotron radiation rocking-curve full width at half-maximum of ~ 30 arcsec) were cut and polished into parallelepipeds for experiments under a DC electric field.

The experiments were performed using *a*-cut and *c*-cut single crystals of L-AHCL.H$_2$O with typical sizes of 4.0 mm $\times$ 2.5 mm $\times$ 1.5 mm and 4.0 mm $\times$ 3.0 mm $\times$ 2.0 mm, respectively. Silver electrodes were painted on the larger face of the crystal. The electric field was generated by a variable-voltage and low-current DC power supply, applied to the samples *via* wires running from the supply to the sample. The maximum electric field applied to the samples was 5×10^4 V m^{-1} (75 V and 100 V for the *a*-cut and *c*-cut samples, respectively). A schematic representation of the crystal set-up is given in Fig. 1.

Renninger scans were carried out in the polarimeter-like diffractometer (Morelhão, 2003) at the XRD1 beamline of the Brazilian National Synchrotron Light Source, Brazil. A parallel-beam geometry was needed to take advantage of the
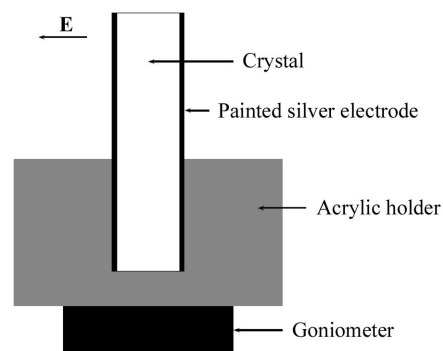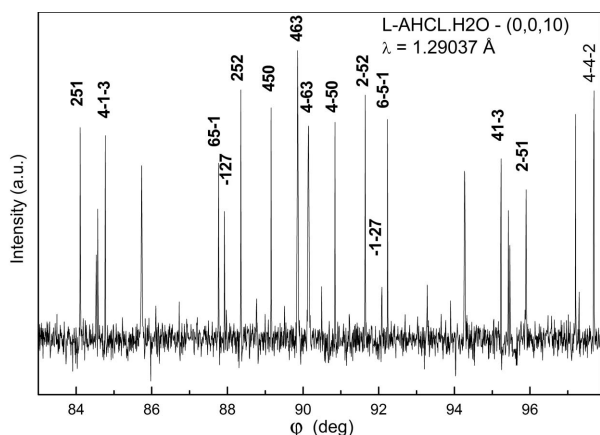

Figure 1
Scheme of the electric field applied in the sample to allow the piezoelectric coefficient determination using three-beam diffraction.

high sensibility of the three-beam diffraction to variation in the lattice parameters. This arrangement usually gives a small photon flux in conventional sources, which restricts the experiments to strong reflections. To overcome this limitation, synchrotron radiation was needed. The energy was tuned to 9608 eV with a bandwidth of 2.5 eV. A 0.5 mm $\times$ 0.5 mm aperture was placed just before the sample to define the beam size as well as the vertical and horizontal angular divergences. The geometry used for the Renninger scans measurements consisted of two channel-cut Si(111) crystals comprising the monochromator. The smallest step-size provided by the experimental set-up was 0.0002° and 0.0005° for the ω and φ axes, respectively. All X-ray three-beam diffraction measurements were carried out at room temperature ($T \simeq 298$ K). The rocking-curve measurements as a function of the electric field for L-AHCL.H$_2$O were performed using a Philips X'Pert MRD system of the X-ray Diffraction Laboratory at UNICAMP, using Cu $K\alpha$ radiation with the tube operated at 40 kV and 40 mA.

4. Results and discussion

The primary reflections for the three-beam diffraction measurements were chosen to be (0,0,10) and (5,0,0) for the electric field applied along X ($\mathbf{E} = E_X\mathbf{x}$) and Z ($\mathbf{E} = E_Z\mathbf{z}$), respectively. As both the primary reflections are weak, all the secondary peaks observed in the Renninger scans are positive (*Umweganregung*). This fact makes it easier to determine the peak position as well as to align the sample. A typical region of the (0,0,10) Renninger scan around the $\varphi = 90°$ symmetry mirror is shown in Fig. 2, while Fig. 3 shows that for the (5,0,0) primary reflection. The indices were determined using the program *mncb* (based on Cole *et al.*, 1962) that had, as input, the lattice parameters, primary reflection and wavelength, generating a table with the peak positions and respective indexes.

By solving equations (1) and (7) the values of the piezoelectric coefficients d_{14} and d_{34} were found to be $(4.0 \pm 0.2) \times 10^{-11}$ C N^{-1} and $(1.1 \pm 0.2) \times 10^{-9}$ C N^{-1}, respectively. Next, putting these values into equations (2) and (8) and plotting the graphs for $(\Delta\gamma + Ed_{14}\cos\beta)(\sin\beta E$ [V m^{-1}]) and $(\Delta\gamma + Ed_{34}\cos\beta)(\sin\beta E$ [V m^{-1}]), as shown in Figs. 4 and 5, the d_{16}

Figure 2
Symmetry mirror of the Renninger scan around $\varphi = 90°$ for the L-AHCL.H$_2$O crystal with primary reflection (0,0,10).
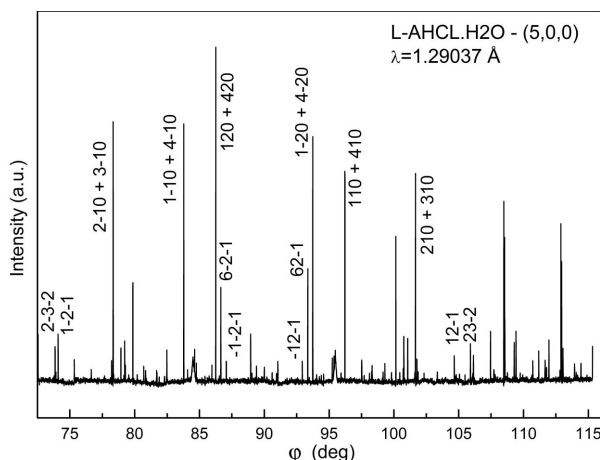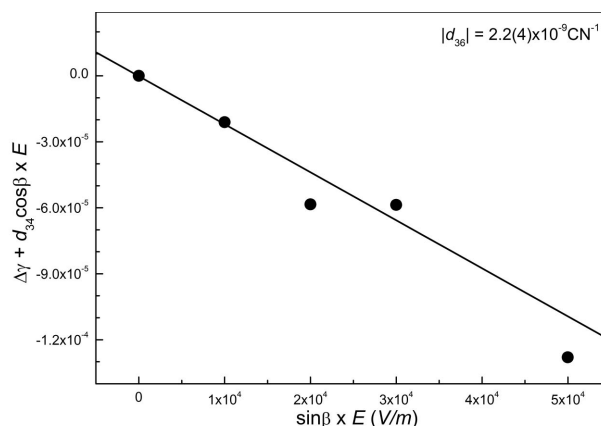

Figure 3
Symmetry mirror of the Renninger scan around $\varphi = 90°$ for the L-AHCL.H$_2$O crystal with primary reflection (5,0,0).
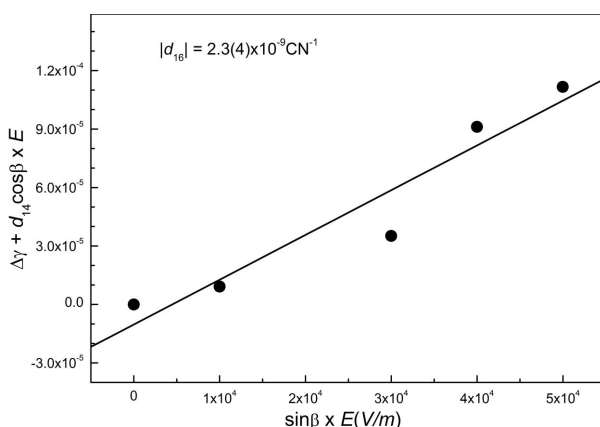
Figure 4
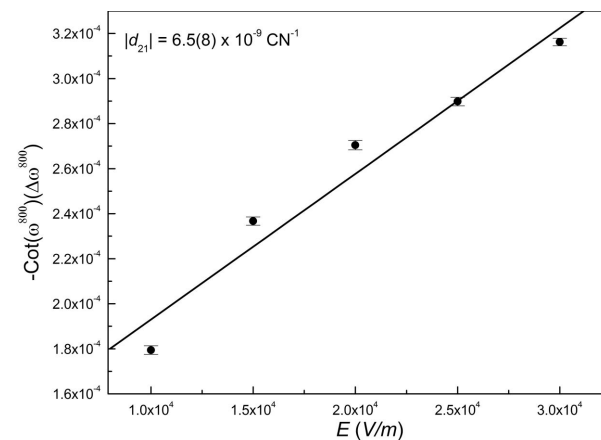Lattice strain *versus* electric field to obtain the d_{16} L-AHCL.H$_2$O piezoelectric coefficient.

and d_{36} piezoelectric coefficients were obtained from the slope of these curves. The results found were $d_{16} = (2.3 \pm 0.4) \times 10^{-9}$ C N^{-1} and $d_{36} = (2.2 \pm 0.4) \times 10^{-9}$ C N^{-1}. All values of the piezoelectric coefficients for L-AHCL.H$_2$O are summarized in Fig. 6.

Figure 5
Lattice strain *versus* electric field to obtain the d_{36} L-AHCL.H$_2$O piezoelectric coefficient.

$$\begin{array}{c} \mathbf{E}_x \\ \mathbf{E}_y \\ \mathbf{E}_z \end{array} \begin{pmatrix} [100] & [010] & [001] & [011] & [101] & [110] \\ 0 & 0 & 0 & 4(2) & 0 & 230(4) \\ 510(5) & 220(3) & 62(8) & 0 & 14(1) & 0 \\ 0 & 0 & 0 & 110(2) & 0 & 220(4) \end{pmatrix} \times 10^{-11} \text{C N}^{-1}$$

Figure 6
Entire piezoelectric coefficients of L-AHCL.H$_2$O obtained using the X-ray three-beam diffraction technique.

Figure 7
L-AHCL.H$_2$O lattice strain $[-\cot(\omega)\Delta\omega]$ obtained from the (800) rocking curve as a function of the electric field $\mathbf{E} = E_Y\mathbf{y}$ providing the d_{21} piezoelectric coefficient.

The (800) reflection was chosen for the rocking-curve measurements to determine d_{21}. Fig. 7 shows the lattice strain $[-\cot(\omega)\Delta\omega]$ as a function of $\mathbf{E} = E_Y\mathbf{y}$; the measured piezoelectric coefficient value was $|d_{21}| = (6.5 \pm 0.8) \times 10^{-9}$ C N^{-1}.

5. Conclusions

The high sensitivity of the X-ray three-beam diffraction method to very small variations in the lattice parameters of a crystal allowed three-dimensional probing of small lattice deformations in L-arginine hydrochloride monohydrate induced by an external electrical field applied parallel to the X and Z axes. Therefore the remaining four piezoelectric coef-

ficients d_{14}, d_{16}, d_{34} and d_{36} were measured. This result can be understood as a useful contribution to the complete piezo-electric characterization of the L-AHCL.H$_2$O crystal since quantitative data is required for technological applications. It should be pointed out that the d_{21} value measured from rocking-curve measurements was in good agreement with our previous results (Almeida *et al.*, 2003), therefore confirming the reliability of the measurements.

References

Almeida, J. M. A., Miranda, M. A. R., Remédios, C. M. R., Melo, F. E. A., Freire, P. T. C., Sasaki, J. M., Cardoso, L. P., dos Santos, A. O. & Kycia, S. (2003). *J. Appl. Cryst.* **36**, 1348–1351.

Avanci, L. H., Cardoso, L. P., Girdwood, S. E., Pugh, D., Sherwood, J. N. & Roberts, K. J. (1998). *Phys. Rev. Lett.* **81**, 5426–5429.

Avanci, L. H., Cardoso, L. P., Sasaki, J. M., Girdwood, S. E., Roberts, K. J., Pugh, D. & Sherwood, J. N. (2000). *Phys. Rev. B*, **61**, 6507–6514.

Chang, S. L. (1984). *Multiple Diffraction of X-rays in Crystals*. Berlin: Springer.

Cole, H., Chamber, F. W. & Dunn, H. M. (1962). *Acta Cryst.* **15**, 138–144.

Deloach, L. D. (1994). *J. Opt. Soc. Am. B*, **11**, 1186–1196.

Dow, J. & Jensen, L. H. (1970). *Acta Cryst.* B**26**, 1662–1671.

Evlanova, N. F., Moldazhanova, G. T., Pashina, Z. S., Rashkovich, L. N. & Shekunov, B. Y. (1990). *Kristallografiya*, **35**, 899.

Haussuehl, S., Chrosch, J., Gnanam, F., Fiorentini, E., Recker, K. & Wall-Rafen, F. (1990). *Cryst. Res. Technol.* **25**, 617–623.

Monaco, S. B., Davis, L. E., Velsko, S. P., Wang, F. T., Eimerl, D. & Zalkin, A. (1987). *J. Cryst. Growth*, **85**, 252–255.

Morelhão, S. L. (2003). *J. Synchrotron Rad.* **10**, 236–241.

Mukerji, S. & Kar, T. (1998). *Mater. Chem. Phys.* **57**, 72–76.

Mukerjia, S. & Kar, T. (2000). *Mater. Res. Bull.* **35**, 711–717.

Nye, J. F. (1957). *Physical Properties of Crystals*. Oxford: Clarendon.

Petrosyan, A. M., Sukiasyam, R. P., Karapetyan, H. A., Terzyan, S. S. & Feigelson, R. S. (2000). *J. Cryst. Growth*, **213**, 103–111.

Rashkovich, L. N. & Shekunov, B. Y. (1991). *J. Cryst. Growth*, **112**, 183–191.

Renninger, M. (1937). *Z. Phys.* **106**, 141.

Santos, A. O. dos, Cardoso, L. P., Sasaki, J. M., Miranda, M. A. R. & Melo, F. E. A. (2003). *J. Phys. Condens. Matter*, **15**, 7835–7842.

Xu, D., Jiang, M. H. & Tan, Z. K. (1983). *Acta Chim. Sin.* **41**, 570–573.